Analysis of a Multilayer Film with Coupled Mode Theory

Silvio Ceccuzzi, Federico Guerra, and Giuseppe Schettini

Abstract – The wave propagation across a one-dimensional electromagnetic band gap (EBG) structure made of alternating layers of material with different dielectric constants is modeled with coupled mode theory. The analytical model, relating the amplitudes of forward and backward waves inside this periodic structure, widely known as multilayer film, is derived and benchmarked with a full-wave code for an extensive subset of the space of parameters. Model validity and advantages are quantitatively analyzed, and some useful capabilities of the adopted approach, beyond the prediction of classical multilayers, are highlighted and explored.

1. Introduction

Natural materials or artificial structures with a space periodic variation of electromagnetic properties act as mirrors for light with a frequency within a specified range. When such a range is in the microwave domain, they are generally referred to as electromagnetic band gap (EBG) materials, and their simplest implementation is the multilayer film, a one-dimensional (1D) periodic stack of dielectric materials with different permittivity. EBGs, and especially multilayer films, are a flourishing, ongoing topic of research because they find large applications in optics and microwave engineering, for instance, in dielectric mirrors and optical filters [1], millimeter-wave components [2], and antennas [3, 4]. Several configurations were studied, such as multiple defects, three or more materials, and gridded layers to tailor the most suitable spectral responses for specific applications [5, 6].

One of the first studies on multilayer film traces back to 1887 with Lord Rayleigh, who analyzed its behavior in terms of multiple reflections and refractions at the boundaries between different materials. Subsequently, multilayer film was simulated with several types of analytical, semianalytical, and numerical approaches, such as transmission line theory, the plane-wave expansion method, time domain techniques, and the finite element method (FEM), just to cite a few [7–9].

In this paper, multilayer film is modeled through coupled mode theory [10], an approximate approach, widely used in many fields, such as power microwaves [11, 12], which describes the physical behavior of the periodic medium in the form of a system of coupled differential equations. The coupled mode theory was applied to several dielectric structures, e.g., in [13], where coupled step-index waveguides were studied, or in [14], where the eigenvalue problem was solved in optical fibers with an inhomogeneous refractive index in the transverse plane. Unlike such works, here a longitudinal variation of the dielectric constant is considered, and profiles other than the classical square wave are also addressed. The theoretical model is validated with a commercial FEM, exploring the range of validity of its approximations over a large set of parameters. A numerical tool extending the capability of the analytical model was developed, achieving noticeable advantages in terms of computation time and physical insight compared with the FEM code. Such advanced capabilities were exploited to design 3D printable multilayer film with a tailored frequency response.

Manuscript received 26 December 2021.

Silvio Ceccuzzi and Giuseppe Schettini are with the Department of Industrial, Electronic, and Mechanical Engineering, Roma Tre University, 62 Via Vito Volterra, Rome, 00146, Italy; e-mail: silvio.ceccuzzi@enea.it, giuseppe.schettini@uniroma3.it

Federico Guerra is with MBDA, 45 Via Monte Flavio, Rome, 00131, Italy; e-mail: federico.guerra.96@gmail.com.

2. Model Description and Validation

In coupled mode theory, the periodic variation of the dielectric constant is dealt as a perturbation current density J_{pert} inserted as an excitation term in the wave equation, which on the basis of Figure 1, takes the following form:

$$\nabla^2 E_y(z) + \omega^2 \mu_0 \epsilon_0 \bar{\varepsilon}_r E_y(z) = i\omega\mu_0 J_{\text{pert}}(z) \qquad (1)$$

where ω, μ_0, and ε_0 are the wave frequency, the vacuum permeability, and the vacuum permittivity, respectively, and a time dependence $e^{\text{i}\omega\text{t}}$ was assumed. The expressions of the electric field and the perturbation current density are

$$E_y(z) = A^+(z)\, e^{-\text{i}\beta\text{z}} + A^-(z)\, e^{\text{i}\beta\text{z}} \qquad (2)$$

$$J_{\text{pert}}(z) = i\omega\epsilon_0[\epsilon_r(z) - \bar{\epsilon}_r]\, E_y(z) \qquad (3)$$

where $\beta = \omega\sqrt{\mu_0 \varepsilon_0 \bar{\varepsilon}_r}$ is the phase constant in a linear isotropic homogeneous material, with the average relative permittivity $\bar{\varepsilon}_r$ of the multilayer film. We are considering normal incidence, but the model can be generalized to the oblique case. In normal incidence, the polarization of the transversal field plays no role, so a y-polarized electric field was assumed without loss of generality.

Two approximations are done in coupled mode theory. The first one is to consider the entire space filled with the periodic medium, which is a rather good approximation as soon as the number of periods of the

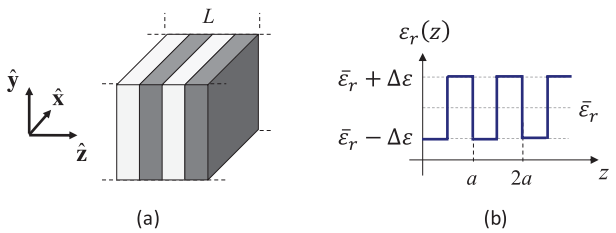

Figure 1. Multilayer geometry (a) and profile of dielectric constant (b).

multilayer is sufficiently high $(L \gg a)$. The second approximation is that the wave amplitudes A^+ and A^- are slowly varying functions of z, so

$$\left|\frac{d^2A^{\pm}}{dz^2}\right| \ll \left|2i\beta\frac{dA^{\pm}}{dz}\right| \tag{4}$$

is always verified, if the perturbation amplitude $\Delta\varepsilon$ is relatively small $(\Delta\varepsilon \ll \bar{\varepsilon}_r)$.

The periodic perturbation of the dielectric constant can be expanded as Fourier series with coefficients

$$b_n = \frac{1}{a}\int_{-a/2}^{a/2}[\varepsilon_r(z) - \bar{\varepsilon}_r]e^{-i\frac{2\pi n}{a}z}dz \tag{5}$$

According to the phase matching condition $\Delta\beta = \beta - \pi/a \approx 0$ [10], the contribution of any coefficient apart from the first one averages to zero. After implementing all premises, the wave equation (1) becomes a pair of first-order differential equations

$$\begin{cases} \frac{dA^+}{dz} = \kappa^* A^- e^{2i\Delta\beta z} \\ \frac{dA^-}{dz} = \kappa A^+ e^{-2i\Delta\beta z} \end{cases} \tag{6}$$

where the asterisk symbol denotes the complex conjugate, and the coupling coefficient

$$\kappa = \frac{ik_0^2}{2\beta}b_1, \tag{7}$$

with $k_0 = \omega\sqrt{\mu_0\varepsilon_0}$, was introduced.

Thus, (6) can be solved either numerically or analytically to derive the reflectance and transmittance of a multilayer film with length L, for the usual boundary conditions $A^+(0) = 1$ and $A^-(L) = 0$. This computation was implemented into a GNU Octave (version 5, free software by J. W. Eaton et al., http://www.octave.org) code and compared with the results of Ansys HFSS (version 2020 R2, Ansys, Inc., Canonsburg, USA), a commercial full-wave code based on the FEM. Two examples of validation are plotted in Figure 2 in terms of the transmittance

$$|T|^2 = \left|\frac{A^+(L)}{A^+(0)}\right|^2 = \left|\frac{S}{iS\cosh(SL) - \Delta\beta\sinh(SL)}\right|^2 \tag{8}$$

where $S = \sqrt{\kappa^2 - \Delta\beta^2}$. Despite the approximations, the coupled mode theory agrees well with the full-wave results for the parameters used in the plot.

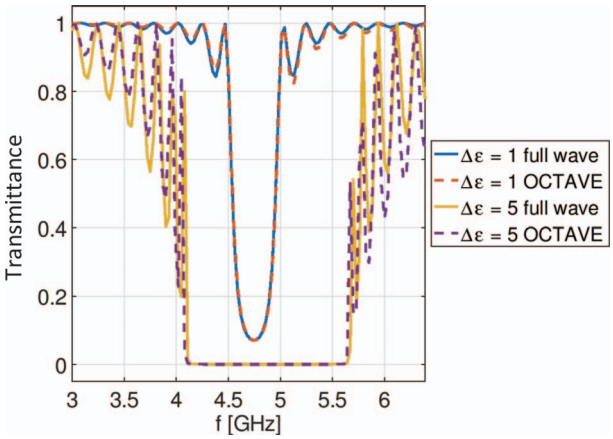

Figure 2. Transmittance of multilayer films with $L = 20a$ and $\bar{\varepsilon}_r = 10$ computed with the code on the basis of coupled mode theory (Octave) and with full wave (HFSS).

3. Tests of Model Reliability and Advantages

The range of validity of model approximations was studied by varying several parameters of multilayer film, such as the average dielectric constant, perturbation amplitude, and number of periods. For all combinations of parameters, the absolute error between the transmittance predicted by our code and HFSS was calculated at each frequency sample over a significant frequency range that includes the transmission peak. The set of error values versus frequency was then averaged, and its variance was calculated to have a performance indicator of model reliability and a measure of the error spread around the average value, respectively.

For the sake of brevity, only a graphical example is reported here in Figure 3. Similar plots were obtained for other combinations of parameters, revealing that the error increases with high perturbation amplitude, small

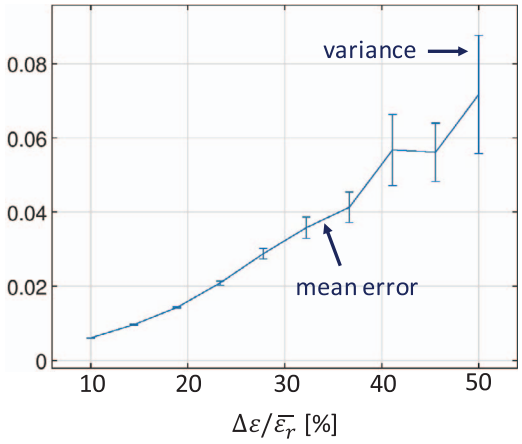

Figure 3. Average absolute error and variance of the transmittance calculated with coupled mode theory and with HFSS versus the perturbation amplitude for a multilayer film with $a = 10$ mm, $L = 20a$, and $\bar{\varepsilon}_r = 10$. Note that the transmittance can vary between 0 and 1.

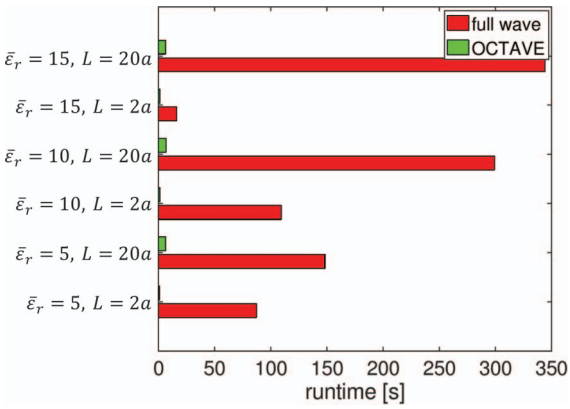

Figure 4. Computation time of 100 frequency points with HFSS and our code for multilayer films with $a = 10$ mm and $\Delta\varepsilon = 0.5\bar{\varepsilon}_r$.

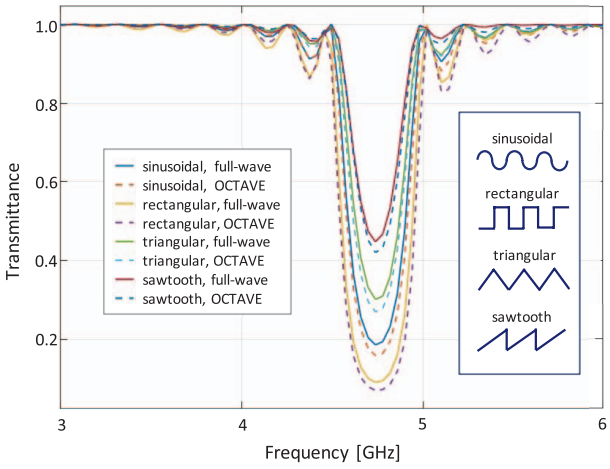

Figure 5. Transmittance versus frequency for 1D dielectric EBG structures with $a = 10$ mm, $L = 20a$, $\bar{\varepsilon}_r = 10$, $\Delta\varepsilon = 1$, and different perturbation profiles.

number of periods, and large number of periods. Such trends can be, respectively, ascribed to the second approximation ($\Delta\varepsilon \ll \bar{\varepsilon}_r$), the first approximation ($L \gg a$), and to numerical accuracy. Note that the error is always low, and for parameter values of practical use, the accuracy is acceptable to carry out the analysis of multilayer films and similar 1D dielectric EBG structures such as those in Section 4.

The use of coupled mode theory in place of full-wave codes appears to be mostly advantageous during the design optimization of the dielectric structures when several simulations or extensive parametric analyses are required. If the analytical solution of (6) is used, the computation is immediate and independent on the input parameters. If the equations are numerically integrated, the developed code is equally much faster than the FEM code by a factor ranging from 20 to 100 for the cases in Figure 4.

4. Applications Beyond the Standard Multilayer Film

A considerable strength of the coupled mode theory is its insight into the modeled physical phenomenon. An example in this sense is the coefficient κ of (7), which determines the coupling level between forward and backward waves inside the multilayer film. The coupling coefficient is proportional to b_1, being the first term of the Fourier series of the periodic profile of the dielectric constant, i.e., the higher b_1, the lower the transmittance of the multilayer film. Alternative periodic profiles can be thus conceived, neglecting the practical implementation that will be addressed later on, and their effectiveness can be easily envisaged. For instance, the following values of b_1

$$\frac{2i}{\pi}\Delta\varepsilon > \frac{1}{2i}\Delta\varepsilon > \frac{4}{\pi^2}\Delta\varepsilon > \frac{1}{\pi}\Delta\varepsilon \qquad (9)$$

sorted in ascending order, respectively, correspond to the rectangular, sinusoidal, triangular, and sawtooth profiles of the dielectric constant. The first term of their Fourier series provides an analytical parameter ruling the performance as can be graphically appreciated from the transmittance curves of Figure 5. The results from both the coupled mode theory and the commercial FEM code are plotted, confirming the trend in (9).

Profiles with continuously varying permittivity, such as the sinusoidal one, can be realized according to the effective medium theory, which describes the macroscopic properties of subwavelength composite materials as homogeneous media [15]. At microwaves, spatial variations of the scale of the wavelength in the permittivity can be engineered starting from a high-permittivity dielectric and introducing thin ($\ll \lambda$) layers of vacuum according to homogenization techniques. This approach can be also adopted to realize the low-permittivity layer ($\bar{\varepsilon}_r - \Delta\varepsilon_r$) of standard multilayer films with a rectangular profile. Most importantly, if the typical permittivity values of 3D printing technology are chosen, the periodic structure with subwavelength slices of dielectric can be manufactured rapidly and at low cost.

The flexibility in realizing complex dielectric profiles, possibly exploiting the advantages of 3D printing, paves the way to conceive advanced multilayer films with tailored frequency response. As an example, a multilayer film consisting in the superposition of two dielectric profiles with different perturbation period is considered. Depending on the value of perturbation periods, the phase matching condition can lead to a broadband or dual-band frequency response. The latter is chosen for this example, aimed at achieving two stopbands at 3 GHz and 5 GHz only alternating layers of vacuum and acrylonitrile butadiene styrene (ABS), i.e., a dielectric material with $\varepsilon_r = 2.9$, widely used in 3D printers, based on fused deposition modeling technology. Figure 6 shows the target profile of the homogeneous effective relative permittivity (Figure 6a), a section of its realistic implementation through ABS slices of various depths (Figure 6b), and the corresponding transmittance curves (Figure 6c). Note that the minimum depth of ABS layers is 0.4 mm, which is

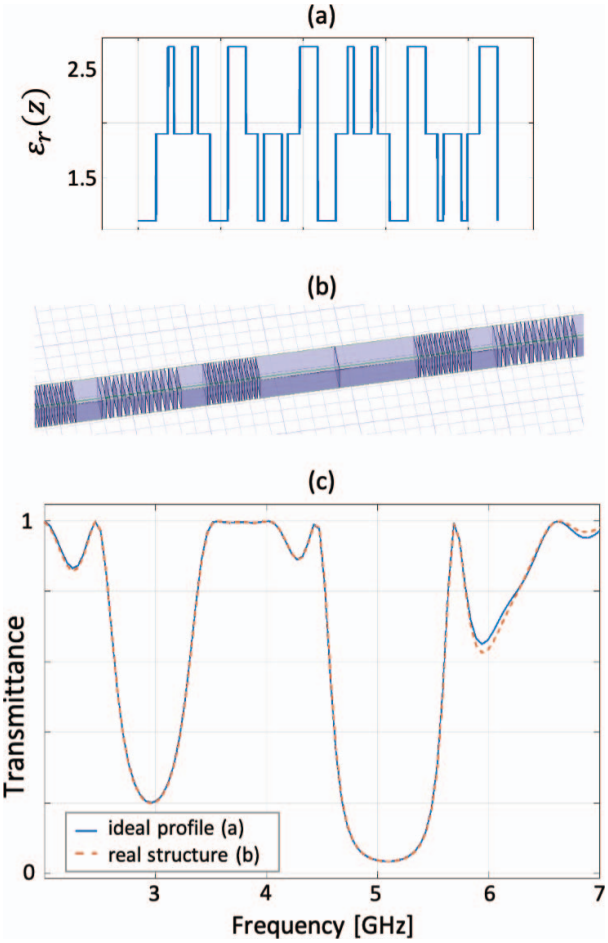

Figure 6. (a) Dual-period perturbation profile of the relative permittivity. (b) Section of the real structure realized by using a single dielectric material with $\varepsilon_r = 2.9$. (c) Transmittance of the structures (a) and (b) with $L = 210$ mm.

around the tolerance of 3D printing technology. Tailored transmittance curves can be achieved increasing the complexity of the dielectric profiles, e.g., adding further periodic perturbation.

5. Conclusions

The coupled mode theory was successfully applied to the study of dielectric 1D EBG (multilayer film). An analytical model was validated, and the range of validity of its approximations was tested over a large set of multilayer parameters, performing a systematic study of error statistics. The model was much faster than a commercial tool on the basis of the FEM. Moreover, it provided a physical explanation about the effectiveness of different types of periodic profiles of the relative permittivity.

The coupled mode theory was also used to explore advanced periodic configurations. A dual-band multilayer structure, which can be manufactured with 3D printers, was conceived, paving the way for the design of tailored dielectric profiles that achieve a desired frequency response. Possible next steps of the present work are the experimental validation of an advanced 3D printable multilayer film or the comprehensive exploration of complex perturbation profiles of the dielectric constant.

6. References

1. E. Hecht and A. Zajac, *Optics*, Boston, Addison-Wesley Publishing Company, 1974.
2. P. de Maagt, R. Gonzalo, Y. C. Vardaxoglou, and J.-M. Baracco, "Electromagnetic Bandgap Antennas and Components for Microwave and (Sub)Millimeter Wave Applications," *IEEE Transactions on Antennas and Propagation*, **51**, 10, October 2003, pp. 2667-2677.
3. H. Yang, J. Lu, C. Lin, C. Song, and G. Gao, "Design of Wideband Cavity-Backed Slot Antenna With Multilayer Dielectric Cover," *IEEE Antennas and Wireless Propagation Letters*, **15**, 2016, pp. 861-864.
4. N. Nguyen-Trong, H. H. Tran, T. K. Nguyen, and A. M. Abbosh, "Wideband Fabry–Perot Antennas Employing Multilayer of Closely Spaced Thin Dielectric Slabs," *IEEE Antennas and Wireless Propagation Letters*, **17**, 7, July 2018, pp. 1354-1358.
5. Y. J. Lee, J. Yeo, R. Mittra, and W. S. Park, "Application of Electromagnetic Bandgap (EBG) Superstrates with Controllable Defects for a Class of Patch Antennas as Spatial Angular Filters," *IEEE Transactions on Antennas and Propagation*, **53**, 1, January 2005, pp. 224-235.
6. C. Ponti, P. Baccarelli, S. Ceccuzzi, and G. Schettini, "Tapered All-Dielectric EBGs with 3D Additive Manufacturing for High-Gain Resonant-Cavity Antennas," *IEEE Transactions on Antennas and Propagation*, **69**, 5, May 2021, pp. 2473-2480.
7. J. D. Joannopoulos, R. D. Meade, and J. N. Winn, *Photonic Crystals: Molding the Flow of Light*, Princeton, NJ, Princeton University Press, 1995.
8. T. F. Eibert, Y. E. Erdemli, and J. L. Volakis, "Hybrid Finite Element-Fast Spectral Domain Multilayer Boundary Integral Modeling of Doubly Periodic Structures," *IEEE Transactions on Antennas and Propagation*, **51**, 9, September 2003, pp. 2517-2520.
9. F. Frezza, L. Pajewski, and G. Schettini, "Full-Wave Characterization of Three-Dimensional Photonic Bandgap Structures," *IEEE Transactions on Nanotechnology*, **5**, 5, September 2006, pp. 545-553.
10. A. Yariv, "Coupled-Mode Theory for Guided-Wave Optics," *IEEE Journal of Quantum Electronics*, **9**, 9, September 1973, pp. 919-933.
11. C. K. Chong, D. B. McDermott, M. M. Razeghi, N. C. Luhmann, J. Pretterebner, et al., "Bragg Reflectors," *IEEE Transactions on Plasma Science*, **20**, 3, June 1992, pp. 393-402.
12. G. L. Ravera, S. Ceccuzzi, G. Dattoli, E. Di Palma, A. Doria, et al., "Optimization of TE_{11}/TE_{04} Mode Converters for the Cold Test of a 250 GHz CARM Source," *Fusion Engineering and Design*, **146**, Part A, September 2019, pp. 745-748.
13. W.-P. Huang, "Coupled-Mode Theory for Optical Waveguides: An Overview," *Journal of the Optical Society of America A*, **11**, 3, March 1994, pp. 963-983.
14. T. DeWolf and R. Gordon, "Complex Coupled Mode Theory Electromagnetic Mode Solver," *Optics Express*, **25**, 23, November 2017, pp. 28337-28351.
15. L. Pajewski, R. Borghi, G. Schettini, F. Frezza, and M. Santarsiero, "Design of a Binary Grating With Subwavelength Features That Acts as a Polarizing Beam Splitter," *Applied Optics*, **40**, 32, November 2001, pp. 5898-5905.